



# DrivingVibe: Enhancing VR Driving Experience using Inertia-based Vibrotactile Feedback around the Head

NENG-HAO YU, National Taiwan University of Science and Technology, Taiwan

SHIH-YU MA, National Taiwan University of Science and Technology, Taiwan

CONG-MIN LIN, National Taiwan University, Taiwan

CHI-AAN FAN, National Taiwan University, Taiwan

LUCA E. TAGLIALATELA, National Taiwan University, Taiwan

TSAI-YUAN HUANG, National Taiwan University of Science and Technology, Taiwan

CAROLYN YU, Information Experience Design Pratt Institute, America

YUN-TING CHENG, National Taiwan University, Taiwan

YA-CHI LIAO, National Taiwan University, Taiwan

MIKE Y. CHEN, National Taiwan University, Taiwan

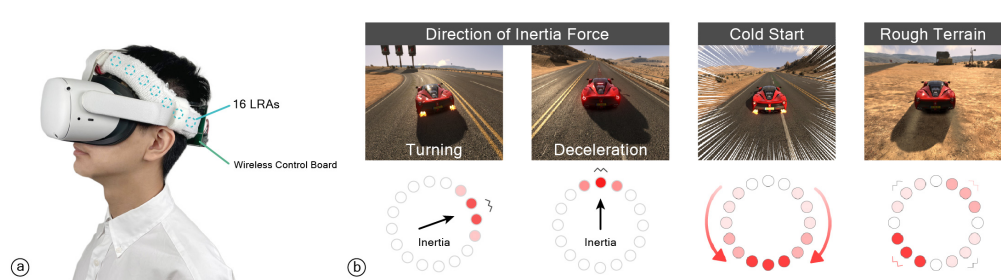


Fig. 1. (a) DrivingVibe vibrotactile headband integrates easily with VR headset to provide (b) inertia-based feedback patterns corresponding to key motion events, including *turning*, *deceleration*, *cold start*, and *rough terrain shaking*.

We present DrivingVibe, which explores vibrotactile feedback designs around the head to enhance VR driving motion experiences. We propose two approaches that use a 360°vibrotactile headband: 1) *mirroring* and 2) *3D inertia-based*. The *mirroring* approach extends the vibrotactile patterns of handheld controllers to actuate the entire headband uniformly. The *3D inertia-based* approach uses the acceleration telemetry data that driving games/simulators export to motion platforms to generate directional vibration patterns, including:

Authors' addresses: Neng-Hao Yu, National Taiwan University of Science and Technology, Taipei, Taiwan, jonesyu@ntust.edu.tw; Shih-Yu Ma, National Taiwan University of Science and Technology, Taipei, Taiwan, leoma0219@gmail.com; Cong-Min Lin, National Taiwan University, Taipei, Taiwan, r10922109@@ntu.edu.tw; Chi-Aan Fan, National Taiwan University, Taipei, Taiwan, r10922159@ntu.edu.tw; Luca E. Taglialatela, National Taiwan University, Taipei, Taiwan, r10922159@ntu.edu.tw; Tsai-Yuan Huang, National Taiwan University of Science and Technology, Taipei, Taiwan; Carolyn Yu, Information Experience Design Pratt Institute, New York, America, cyux16@pratt.edu; Yun-Ting Cheng, National Taiwan University, Taipei, Taiwan, r09922063@g.ntu.edu.tw; Ya-Chi Liao, National Taiwan University, Taipei, Taiwan, b07901104@ntu.edu.tw; Mike Y. Chen, National Taiwan University, Taipei, Taiwan, mikechen@csie.ntu.edu.tw.

Permission to make digital or hard copies of all or part of this work for personal or classroom use is granted without fee provided that copies are not made or distributed for profit or commercial advantage and that copies bear this notice and the full citation on the first page. Copyrights for components of this work owned by others than ACM must be honored. Abstracting with credit is permitted. To copy otherwise, or republish, to post on servers or to redistribute to lists, requires prior specific permission and/or a fee. Request permissions from permissions@acm.org.

© 2023 Association for Computing Machinery.

2573-0142/2023/5-ART206 \$15.00

<https://doi.org/10.1145/3604253>

i) centrifugal forces, ii) horizontal acceleration/deceleration, and iii) vertical motion due to rough terrain. The two approaches are complementary as the *mirroring* approach supports all driving games because it does not require telemetry data, while the *3D inertia-based* approach provides higher feedback fidelity for games that provide such data. We conducted a 24-person user experience evaluation in both passive passenger mode and active driving mode. Study results showed that both DrivingVibe designs significantly improved realism, immersion, and enjoyment ( $p < .01$ ) with large effect sizes for the VR driving experiences. For overall preference, 88% (21/24) of participants preferred DrivingVibe, with a 2:1 preference for *3D inertia-based* vs. *mirroring* designs (14 vs. 7 participants). For immersion and enjoyment, 96% (23/24) of participants preferred DrivingVibe, with nearly 3:1 preference (17 vs. 6 participants) for the *3D inertia-based* design.

**CCS Concepts:** • Human-centered computing → Virtual reality.

**Additional Key Words and Phrases:** Games/Play ; Haptic ; Virtual Reality ; Sensorimotor Contingency ; Motion simulators ; Head Vibrations

#### ACM Reference Format:

Neng-Hao Yu, Shih-Yu Ma, Cong-Min Lin, Chi-Aan Fan, Luca E. Taglialatela, Tsai-Yuan Huang, Carolyn Yu, Yun-Ting Cheng, Ya-Chi Liao, and Mike Y. Chen. 2023. DrivingVibe: Enhancing VR Driving Experience using Inertia-based Vibrotactile Feedback around the Head. *Proc. ACM Hum.-Comput. Interact.* 7, MHCI, Article 206 (May 2023), 22 pages. <https://doi.org/10.1145/3604253>

## 1 INTRODUCTION

Haptic feedback enhances the realism, immersion, and enjoyment of virtual experiences [37, 39, 42, 62], with all current VR platforms and popular game consoles supporting controller-based vibrotactile feedback. To enhance motion experiences, such as driving and flying, traditional motion platforms mechanically tilt and move the entire person, which requires large machinery [22]. Even with the significant space and cost requirements, interest in consumer motion platforms has been growing rapidly along with VR headsets, particularly for driving and flight simulation. A survey of two popular consumer motion platforms shows that they support 50 and 67 driving games, respectively.<sup>1</sup>

To address the limitations of motion platforms, researchers have explored more compact designs as well as wearable approaches to motion simulation. HapSeat [9] used three 3-DOF motorized actuators attached to seats to independently move users' heads and hands instead of the entire body. HeadBlaster [37] introduced the first wearable motion simulator by integrating air propulsion jets into VR headsets, but it requires being tethered to large, costly air compressors. Odin's Helmet [24] used head-mounted high-speed propellers instead of air jets, but generates unsafe noise that exceeds 100dB for the user (up to 108dB) and people nearby, which could lead to hearing loss in 5 minutes according to CDC [14]. While these approaches eliminate the need for large mechanical platforms, significant barriers to consumer adoption remain, such as mobility, noise, space, and cost.

Vibrotactile actuators, particularly Linear Resonant Actuators (LRAs), have been embedded in VR controllers and smartphones to provide haptic feedback. They are compact, low-cost, and lightweight and have been integrated into research head-mounted devices [7, 10, 11, 29, 31, 32, 64], commercial head-mounted devices [3], and are starting to be integrated into next-generation VR headsets, such as PlayStation VR2 (2023) [13].

While prior research has explored using head-mounted vibrotactile actuators for a wide range of use cases, including directional cues for navigation and guidance [29, 64], notifications [30], simulating raindrops [10], and enhancing instantaneous teleportation in VR [7], none have explored designing vibrotactile feedback to enhance continuous motion experiences, such as driving.

---

<sup>1</sup>Support of driving games by popular consumer motion platforms, as of May 1, 2023: 1) Next Level Racing (50 games): <https://nextlevelracing.com> and 2) Motion Systems (67 games): <https://motionsystems.eu>

We present DrivingVibe, which explores how vibrotactile feedback patterns around the head can be used to enhance VR driving experiences. We propose two approaches and designs using 360°vibrotactile headbands: 1) *mirroring* and 2) *3D inertia-based* designs. The *mirroring* approach extends the vibrotactile patterns of the handheld controllers to actuate the headband uniformly. This black-box approach does not require any motion telemetry data, and can easily support all existing virtual driving experiences that have haptic feedback. The *3D inertia-based* approach uses the telemetry data exported by virtual driving games and experiences for the motion platform, in order to provide directional vibration patterns corresponding to the direction of inertial forces in 3D, i.e., X, Y, and Z axes. The two approaches are complementary as the *mirroring* approach supports all driving games that support controller-based vibration, while the *3D inertia-based* approach provides higher feedback fidelity for the games that provide telemetry data.

Using a headband with 16 Linear Resonant Actuators (LRAs), we designed feedback patterns for motion events that correspond to significant inertial and centrifugal forces and also when transitioning between stationary and mobile, when the human perception of motion is the most sensitive due to sensory adaptation [39]. Specifically: 1) turning, 2) acceleration/deceleration, which includes crashing, 3) cold start, and 4) vertical motion caused by rough terrain. Based on sensorimotor contingencies [12, 67], which refers to the matching of particular patterns from multisensory information to actions, we designed the *3D inertia-based* feedback using the following two types of vibrotactile patterns: 1) *directional cues* using a subset of actuators, and 2) *motion cues* using apparent tactile motion [7], as shown in Figure 1.

We completed three device design iterations to improve the usability of our prototype, then conducted a 24-person summative study to evaluate the VR driving experience of these feedback designs. The user study consisted of both passive passenger mode and active driving mode, with the latter using handheld controllers with vibrotactile feedback. Study results showed that both DrivingVibe designs significantly improved realism, immersion, and enjoyment ( $p < .01$ ) with large effect sizes in both modes of VR driving experiences. In terms of overall preference, 88% (21 out of 24) of participants preferred DrivingVibe, and among those, users preferred the *3D inertia-based* design with a ratio of 2:1 (14 vs. 7 participants). Furthermore, DrivingVibe is lightweight, compact, and low-cost, and the entire system can be integrated into VR headsets, making it practical for researchers to experiment with and for consumer adoption. We are open-sourcing the entire software and hardware of DrivingVibe so that others can experience and build upon our progress.<sup>2</sup>

The rest of the paper first reviews related research on motion simulation and applying haptic feedback to the head. We then discuss the vibration pattern designs and implementation and present user experience evaluation and discussion.

## 2 RELATED WORK

Our work is inspired by the rich body of prior work on motion simulation and head-based haptic feedback.

### 2.1 Motion Simulation Techniques

Historically, motion platforms were originally invented at the beginning of the 1900s for training pilots. Over time the actuation methods evolved from manual [22], to wind-based [52], to linear actuators [58], and their number of supported degrees of freedom (DoF) increased from 3-DoF (pitch, roll, and yaw) [1] to 6-DoF (rotational: pitch, roll, and yaw, translational: surge, heave, and sway) [58]. While motion platforms continue to be indispensable for training [2, 16], they

<sup>2</sup>Open source URL: <https://github.com/ntu-hci-lab/DrivingVibe>

have also become popular for entertainment [54] and for personal VR experiences, particularly for driving [23] and flight simulation.

To reduce the space and machinery required by large, mechanical motion platforms, seat-based approaches such as HapSeat [9] and vibrotactile actuators have been explored for motion [8, 21, 35, 55, 69] and terrain texture [36, 38] simulation.

Headset-based motion simulation using compressed air jets, such as HeadBlaster [37] and HeadWind [62] have been shown to increase realism and immersion of motion and teleportation in VR, respectively. These approaches, however, require a source of compressed air provided by air compressors or portable air tanks. Odin's Helmet [24] uses head-mounted propellers that produce noise >100dB for the user (up to 108dB) and people nearby (up to 104dB) which can lead to hearing loss in 5 minutes, according to the US Centers for Disease Control and Prevention (CDC) [14].

There have also been studies that aim to exploit illusory effects to induce a sense of motion. Välijamäe et al. [63] used auditory scene cues to create an illusory sense of user movement relative to the source of the sound. Pittéra et al. [48] used ultrasound haptics to induce an intermanual tactile illusion of movement, but requires ultrasonic transducer arrays that are not mobile.

This paper takes a novel approach to enhance motion experience by designing around-the-head vibrotactile feedback patterns. While vibrotactile actuators are limited in power and fidelity compared to larger, heavier, and nosier actuators, we explore two pattern designs that significantly enhance the driving motion experience.

## 2.2 Haptic Feedback on the Head

Kabuto [61] and GyroVR [19] rendered impact and inertia through the use of head-worn flywheels and their gyroscopic effects. VaiR [51], AmbioTherm [49], ThermEarhook [45] and VWind [25] increased sense of presence and immersion using head-focused thermal and wind stimuli. Head-based force feedback [5], electrical-muscle-stimulation (EMS) [59, 60], lateral skin stretch [65], and 3-DoF rotational cues based on shear forces [33] among others have also been explored. Researchers have also explored feedback that focuses on the face, such as Face/On [10], FaceHaptics [66], Virtual Whiskers [44], HeadWind [62], and Mouth Haptics [56]. While diverse in the types of haptic feedback, some of these prior approaches require significant hardware to be mounted on the headset, and have not explored haptic designs for continuous motion simulation, such as driving.

Additionally, previous research has demonstrated that humans can accurately recognize spatial vibrotactile patterns around the head [11, 30], which can be used to guide them towards visual targets in virtual environments [6]. Furthermore, vibrotactile funneling illusion, which is the sensation of a single (non-existing) stimulus somewhere in-between the actual stimulus locations, has been observed around the head [32]. ProximityHat [40], HapticHead [28, 29, 31], and TactiHelm [64] around-the-head directional cues for navigation in real world and virtual environments, and MotionRing [7] showed how apparent tactile motion can be created on the head to enhance VR experiences, such as instantaneous teleportation and objects flying by. While these approaches have explored vibrotactile and directional cues, they have not explored haptic designs for inertia forces nor continuous motion simulation.

Inspired by these prior works, this paper contributes a design exploration using practical, headset-integrated vibrotactile actuators to enhance continuous motion experience, specifically driving.

## 3 DEVICE DESIGN AND IMPLEMENTATION

To design and evaluate vibrotactile feedback patterns around the head, we used an iterative design process to improve the usability of our prototype device and also the vibrotactile pattern designs. We present our device design in this section and vibrotactile feedback design in the next section.

### 3.1 Device Design

We reviewed several types of vibrotactile actuators, including eccentric rotating mass (ERM), linear resonant actuator (LRA), Dielectric elastomers actuators (DEA), and piezoelectric actuators. ERM and LRA are the most commonly used actuators used in a gamepad and VR controllers and prior research headset devices [7, 47]; thus we selected them for availability, low noise, low cost, and ease of integration into VR headsets.

**3.1.1 Device: V1 (4 x ERM).** As shown in Figure 2(a), our first prototype consists of 4 ERM motors (Parallax, 12mm coin type, 9000rpm) pressed into the sponge cushion of the Vive Pro HMD, controlled via an Arduino Nano board on the front of the HMD. It supports vibrotactile feedback in 8 directions by actuating one or two of the motors. However, we found the resolution of directionality was too limiting.

**3.1.2 Device: V2 (16 x LRA).** For higher haptic resolution, we referenced the findings of MotionRing [7], which demonstrated that apparent tactile motion (ATM) is feasible on both 12-LRA and 16-LRA headband designs. We used the 16-LRA design for higher haptic resolution, which has an angular spacing of 22.5°. We initially used the same coin-type LRA as MotionRing but found that these LRAs often malfunctioned due to overheating in extended, continuous usage for driving. Therefore, we switched to the LRAs used by Nintendo Switch controllers (VL91022-170H, 22.6mm x-axis rect type), which can sustain extended actuation and also has the benefit of 10x larger amplitude of 2.3N (vs. 0.2N).

As shown in Figure 2(b), the 16 LRAs are controlled via 16 DRV2605L driver boards by a NodeMCU-32S on a perfboard, which was encased in an acrylic case and attached to the back of the VR headset. The LRA headband weighs 180g, while the board with the case weighs 262g and has a volume of  $17 \times 9.5 \times 3.5 \text{ cm}^3$ .

**3.1.3 Device: V3 (Wireless).** Based on feedback from the V2 version, we made three key improvements to make the device easier to wear and operate, as shown in Figure 2(c) and also Figure 1(a). First, we reduced the weight and volume of the control board by more than 80% to 45g and more than 70% to  $10 \times 7.5 \times 2 \text{ cm}^3$ , by custom designing a printed circuit board (PCB) to simplify the wiring. Second, we made the system wirelessly controlled via Wi-Fi, enabling full user mobility. Third, we improved the mounting of LRAs to the headband with double-sided tape, preventing unintended rotation during wearing and usage, which sometimes caused the LRA's actuating axis to deviate from being perpendicular to the surface of the head resulting in unpredictable intensity.

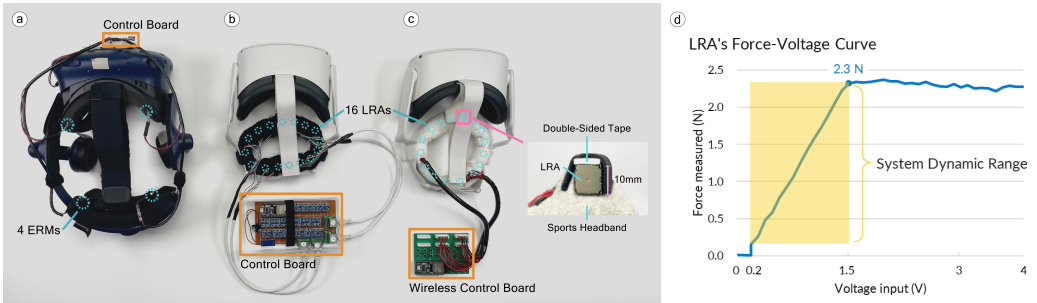


Fig. 2. (a) V1 prototype with 8 ERMs; (b) V2 prototype with 16 LRAs; (c) V3 wireless device used in user experience evaluation; (d) Force output vs. input voltage for the LRA

### 3.2 LRA Amplitude and Response Time

We controlled the LRA voltage from 0-5V [57] and measured the force output using a IMADA ZTS-20N load cell, which can record data at 2000Hz at up to 20N and has a rated accuracy of 0.2% full scale (0.04N). As shown in Figure 2(d), the LRA generates force amplitude at 1.5N per volt input ( $R^2 = 0.999$ ) from 0.2N up to 2.3N, which we use as the controllable dynamic range of the system.

The response time of the LRA to reach maximum amplitude is 10ms. The system updates the vibration state of the headband at a rate of 25Hz, resulting in a maximum total response time of 50ms, which is much faster than the 100ms tactile simultaneity threshold so that no latency would be perceived by users [15, 50].

### 3.3 Motion Telemetry and Controller Data

Games support motion platforms by exporting motion information in real-time via motion telemetry API. Because we are effectively building a wearable motion simulator, we use the same mechanism to read the in-game motion data through the telemetry API via a UDP port [37]. We developed a Unity3D program (2019.4.10f) that: 1) reads lateral acceleration, suspension height information, and controller feedback intensity; 2) computes the corresponding feedback patterns; 3) converts the pattern to binary data that specifies the output intensity of each of the 16 LRAs, compensating for the HMD heading due to head rotation; and 4) sends the data to the control board via Wi-Fi.

To access the controller haptic feedback intensity, we used the Virtual Gamepad Emulation Framework [46] to create a virtual controller acting as a relay between the physical controller and the games.

### 3.4 LRA Calibration

Because the actuators are placed around the head, the same LRA intensity may be perceived differently due to factors such as hair and curvature [43]. Furthermore, even the same batch of LRAs will have slight variances in their output. To ensure that each LRA is perceived to have identical intensity by the user, we developed a calibration process and iteratively improved it.

Our current calibration process uses a 2-phase design. In the first phase, the front center LRA is used as the baseline, and users use an Xbox wireless controller's D-pad to move the target LRA to be calibrated (left/right) and adjust its intensity (up/down) to match the baseline. The baseline LRA and the target LRA would alternately vibrate for 0.5 seconds, ensuring that users can clearly perceive each LRA's intensity. The second phase is verification. The system iterates through all LRAs for users to double-check their calibration, and users can adjust as necessary.

After completing calibration, we record all the intensity adjustments for each LRA. The adjustments are then normalized by dividing each by the maximum and then stored as percentage weights that will be multiplied when computing the final output. The calibration process typically takes 3-5 minutes and only needs to be performed once per user.

## 4 VIBROTACTILE PATTERN DESIGN

### 4.1 Design Process

We explored and iteratively refined our inertia-based designs. We will briefly summarize the design iterations but will focus on describing the current pattern design in detail in the rest of the section.

### 4.2 3D Inertia-based Approach

The initial goal is to enhance the motion experience using directional cues. Directional cues are essential in enhancing motion experience because they provide users with information about the direction and intensity of motion, which can help them better understand and anticipate the motion

of objects in their environment [6]. By providing directional cues through vibrotactile feedback, users can more easily perceive the motion and feel more immersed in the experience. To achieve this, we propose a *3D inertia-based* approach that focuses on mapping vibrotactile patterns to inertia experiences during motion. The aim of this approach is to develop a feedback pattern that generates vibration patterns that can be intuitively associated with motion events through sensorimotor contingency [34]. The following describes the key types of motion events and the algorithms to generate corresponding vibrotactile patterns.

**4.2.1 Motion Events for Driving.** Human interprets head and body motion by integrating inputs from our vestibular (semicircular canals and otolith organs), somatosensory (specifically proprioception), and visual systems [17]. Prior work on motion simulation [37] has identified inertia forces due to lateral acceleration/deceleration and turning as key motion events. For driving in particular, there are additionally two notable motion events: 1) change in vehicle suspension height caused by rough terrain that leads to perceivable vertical motion, and 2) acceleration from a stationary state which is more noticeable vs. from a moving state. In summary, the four types of key motion events, as shown in Figure 5, are: 1) cold start, 2) acceleration/deceleration, 3) turning, and 4) rough terrain. It is worth noting that vehicle collisions and crashing are examples of deceleration events.

#### 4.2.2 Pattern Design of Motion Events.

**Directional Cue Design for Acceleration/Deceleration/Turning.** Since *deceleration*, *acceleration*, and *turning* are perceived as inertia with different directions and magnitudes, we use directional cues to represent the direction and intensity of the inertia force vector. Inspired by prior work such as HapticHead [29] that used 3-actuator vibration to render the direction of surrounding objects, we adapted the concept for driving scenarios and conducted several pilot tests for different ranges of area, we found that 90° of actuation range is both noticeable and comfortable.

After compensating for HMD heading relative to the vehicle heading due to head rotation, the function to compute intensity  $I$  for a motor for any given inertia vector is calculated as follows:

$$I_{motor} = \max \left( 0\%, \min \left( 100\%, \frac{G_{now} - G_{lower}}{G_{upper} - G_{lower}} \right) \right) \times \left( 100\% - \frac{\min(|\theta|, 45^\circ)}{45^\circ} \right)$$

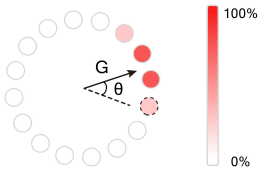


Fig. 3. Schematic diagram of the directional cue design.

$G_{lower}$  and  $G_{upper}$  stand for the lower threshold and the upper threshold to the magnitude of inertia, and  $\theta$  stands for the angular distance from any certain motor to the direction of the inertia vector. In order to determine the appropriate thresholds for our feedback, we analyzed the dynamic ranges of the inertia observed in the Assetto Corsa game. Based on this analysis, we set a lower threshold of 0.1 g ( $\approx 0.98m/s^2$ ) and an upper threshold of 1.3 g ( $\approx 12.74m/s^2$ ) for our feedback. While the upper threshold defined when to max out the feedback intensity, the lower threshold could screen out the subtle noise to prevent over-stimulation caused by overly frequent actuation. We used linear interpolation when the inertia was at intermediate values. The vibrators with

an angular distance less than  $45^\circ$  will be activated with another interpolation on the intensity according to their angular distance to the direction of the inertia vector, i.e. the closer the vibrator is to the inertia direction, the higher its intensity, as shown in Figure 3.

*Feedback Design for Suspense Height Changes over Rough Terrain.* Suspension height is the distance between the lowest point of a tire (normally contacting the ground) and the underside of the vehicle chassis. To estimate the vertical acceleration for each suspension, we calculate the derivative of the suspension height independently for the four tires. We split the actuators into 4 regions corresponding to the directions of the 4 tires. For example, the 3 front-right actuators correspond to the front-right tire, as shown in Figure 1(b). The four actuators at the exact front, back, left, and right are not used to provide better separation between the 4 regions.

The function to calculate intensity is given by, after which the patterns are mapped to physical LRAs by compensating for HMD heading relative to the vehicle heading due to head rotation:

$$I_{motor} = \max \left( 0\%, \min \left( 100\%, \frac{\frac{dH}{dt} - H_{lower}}{H_{upper} - H_{lower}} \right) \right)$$

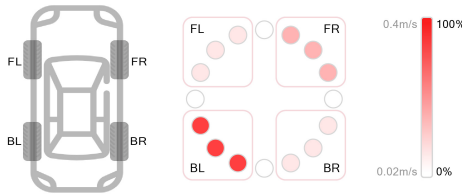


Fig. 4. Schematic diagram of the directional cue design

Similar to the *Directional Cue* design,  $H_{lower}$  and  $H_{upper}$  stand for the thresholds to prevent overstimulation and set the max intensity. For the Assetto Corsa game, we set the lower threshold to 0.02 m/s so that the actuators stay static when driving on the smooth track and start to vibrate when driving on rough terrains such as grass fields. The intensity is again linearly interpolated for those between the two thresholds. (Figure 4)

*Apparent Tactile Motion for Cold Start.* Apparent Tactile Motion (ATM) is an illusion when two sequential tactile stimuli presented at separate locations on the skin produce an illusion of a tactile movement between the two points. [4]. The speed of motion can be controlled through timing, distances, and intensity. Inspired by MotionRing [7] that used tactile motion to simulate air drag, we extend its ATM design to support continuous ATM, and explore how it can be used to improve driving motion experience.

We experimented with ATM in various virtual driving experiences, such as high velocity, high engine RPM, and forward acceleration. However, while users initially liked ATM, they started to report over-stimulation after extended exposure to such feedback. Based on feedback from users, we use ATM only during *cold start* (i.e. forward acceleration from a stationary state), which is when users are the most sensitive to acceleration and expect a corresponding strong feedback. Figure 5(d) shows an example of ATM patterns during a cold start.

For the Assetto Corsa game, we set the threshold of the *cold start* event as acceleration of more than half-throttle while the velocity is less than 5 m/s. We set the ISOI at 100 ms according to the perceptual model from MotionRing [7], resulting in an angular speed of 0.625 rps. The duration is set to 300 ms or three-motor overlap in a single ATM. When the *cold start* events are detected, ATMs would be constantly produced at a rate of twice per second, or every 500 ms, from the front center and then traverse through both sides of the head. We defined the interval by specifying the angular gap between two consecutive ATMs, so 500 ms resulted in a 45°gap or two motors of spacing, which was needed to perceive two distinct ATM patterns.

Overall, because it is possible for the above three patterns to occur at the same time, all patterns are calculated independently and the intensities are summed, i.e. if a motor is responsible for multiple patterns, each pattern's intensity for that motor would be summed up for its final output intensity.

### 4.3 Mirroring Approach

Since the 3D inertia-based approach relies on in-game motion data, which is either provided by game developers or obtained through telemetry APIs, we found that most driving games already have some form of controller-based haptic feedback that vibrates at similar key events as those mentioned earlier. Thus, we developed the mirroring approach, which leverages the existing controller-based haptic feedback to provide the same feedback to the headband. It's a black-box approach that can support games that do not export motion telemetry data. Using one of the top-rated VR racing games, Assetto Corsa <sup>3</sup>, as an example, we analyze its vibration feedback patterns and describe how we map them into feedback patterns for the headband.

**4.3.1 Controller-based Haptic Feedback in Racing Games.** Modern gamepads and VR controllers use two vibrotactile actuators to deliver a richer haptic experience than a single actuator. For example, each Xbox ONE controller has two ERM motors, and each DualSense™ wireless controllers use two LRA motors. VR controllers and Nintendo Switch Joy-Con controllers have an LRA in each of the left- and right-hand controllers. Because most VR and console controllers/gamepads have haptic motors installed in a left-right manner, applications typically specify the intensity of the left and right motors which will function across hardware platforms.

The Assetto Corsa game is highly rated for its advanced physics engine and realistic visuals, and we analyze how it actuates the motors in the Xbox ONE controller, which has a low-frequency ERM motor on the left side and a high-frequency one on the right side. As shown in Figure 5(a)(b), the left (low-frequency) motor is actuated only when the vehicle goes outside the track into rough terrain and the right (high-frequency) motor is actuated for all other events such as accelerating, decelerating, and turning. While the intensity of the right motor varies to reflect the magnitude of the G-force, the left motor is actuated at either 0% or 100% intensity.

**4.3.2 Headband Intensity Mapping.** Because the left and right haptic feedback do not contain directionality information, we take a straightforward approach to calculate intensity by averaging the intensity levels of the left and right motors, and vibrate the entire headband uniformly. Figure 5(b)(c) visualizes how the vibration feedback intensity is the average of the two motor intensities over different driving events.

---

<sup>3</sup>Assetto Corsa on SteamVR [https://store.steampowered.com/app/244210/Assetto\\_Corsa/](https://store.steampowered.com/app/244210/Assetto_Corsa/)

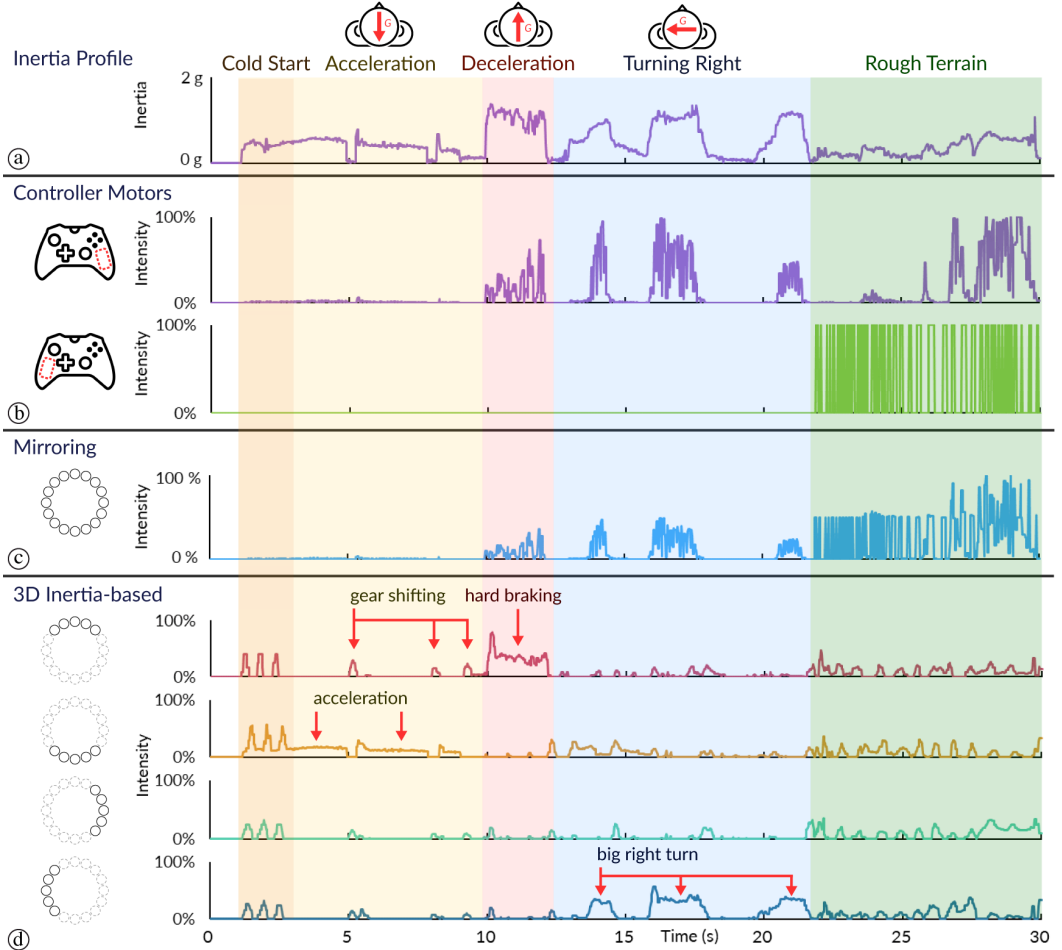


Fig. 5. Visualization of inertia forces and haptic patterns across 5 types of motion events: (a) inertia magnitude; (b) The left/right controller haptic feedback intensity provided by the driving game; the right motor corresponds to inertia, and the left motor corresponds to rough terrain; (c) The corresponding DrivingVibe motor intensity in the *mirroring* mode; (d) The corresponding DrivingVibe motor intensity in the *3D inertia-based* approach. To better show the directionality of this approach, the average intensity of the four quadrants is shown individually. Note: The inertia and intensity values were obtained via the Telemetry API and game controller API.

## 5 USER EXPERIENCE EVALUATION

To evaluate the user experience of DrivingVibe designs, we selected one of the top-rated VR racing games, Assetto Corsa<sup>4</sup>, that supports telemetry API, has realistic audio-visual, physics engine, and well-designed haptic feedback. We debated between using a steering wheel vs. gamepads for input and haptic feedback. While steering wheels and gas/brake pedals are used by serious gamers and driving enthusiasts, the majority of players will be experiencing virtual driving using the default gamepads and controllers.

<sup>4</sup>Assetto Corsa on SteamVR [https://store.steampowered.com/app/244210/Assetto\\_Corsa/](https://store.steampowered.com/app/244210/Assetto_Corsa/)

## 5.1 Experimental Design

This study uses a within-subjects experimental design to compare user experiences. The independent variables has three levels which resulted in the three conditions: two DrivingVibe feedback patterns, *mirroring* and *3D inertia-based* designs, vs. a baseline. To ensure that each participant experiences a controlled set of the exact same motion events, we designed the study to be in passenger mode first, followed by free play in active driving mode to capture the experience of playing a driving game. In driver mode, the built-in controller vibration is used as a well-designed baseline, as well as the input source for the *mirroring* mode. In passenger mode, the baseline is no haptic feedback as users are passive observers and controllers are not used.

We created a total of four tasks. The first three tasks are designed for users to experience specific types of motion events: 1) acceleration and deceleration (including cold start), 2) turning, and 3) rough terrain. These three are designed to be in passenger mode, in order to carefully control that all users experience the exact same motion experience. The fourth task involved active free play in driver mode, where users could freely drive around the course and experience a mix of different sensations.

For each task, users experience the 3 feedback conditions, in counter-balanced ordering. After each condition, users rated its immersion, realism, enjoyment, and comfort on a 7-point Likert scale. Likert scales were used to evaluate the overall perceived user experience, rather than how well the physical properties of inertia were simulated. Specifically, the immersion and realism questions were adapted from the Presence Questionnaire (version 3)'s [68] questions 18 and 8.

After completing all conditions for all tasks, users chose their most-preferred condition for immersion, realism, enjoyment, and overall preference. We prepared semi-structured interview questions to understand how the two pattern designs did or did not meet their expectations. We also asked them about the influence of the motor sound and whether they noticed the directionality feedback and tactile motion patterns.

**5.1.1 Tasks 1-3: Passenger Mode.** To ensure that all participants experienced the exact same motion events, we implemented the passenger experience by using prerecorded clips with the replay function supported by the game. All 3 tasks started with the car being stationary and ended with braking to complete stop. The duration was chosen to be one minute to minimize motion sickness.

- Acceleration/Deceleration: was recorded on the Drag 2000m track. It included two full-throttle accelerations, two half-throttle accelerations, two full-brake decelerations, and two half (50%) braking decelerations.
- Turning: was recorded on the Vallelunga - Club track. It included two right turns and three left turns, spending about 33% of the time in the turns.
- Rough Terrain: was recorded on the Mugello Circuit track. The car was driving onto the grass field and then back on the road for four times, spending about 50% of the time on the grass field.

**5.1.2 Task 4: Driver Mode.** For free driving, we selected the Mugello Circuit track which has 15 turns and a long straight section, and the Lotus Elise SC car in gamer mode. A sample VR scene is shown in Figure 6(c), and to reflect a typical gaming experience, the controller vibration feedback is on for all conditions. The task duration was extended to two minutes to allow participants time to experience different driving motions.

## 5.2 Participants and Procedure

We recruited 24 participants, 14 males and 10 females with age 20-43 (mean = 24.6, SD = 4.5), with Motion Sickness Susceptibility Questionnaire (MSSQ) scores below 70, which is the 80th

percentile [18] to ensure that participants could finish the experiment without dropping out due of motion sickness. Participants all had normal or corrected-to-normal vision and had at least five real-world driving experiences in the past year. The experiment took approximately one hour and each participant received the equivalent of USD\$6.5 compensation.

Upon participants' arrival, we explained the study procedure and measured their interpupillary distance (IPD) for HMD adjustment. We assisted participants to put on the Oculus Quest 2 HMD and the vibrotactile headband, in a seated position, as shown in Figure 6(b)(d). The driving game ran on a PC with an i5-11300H CPU, NVIDIA GeForce RTX 3060 Laptop GPU, and 24GB RAM. The study was conducted with the game's default sound effects without no background music to ensure that the experiment was close to a real driving experience.



Fig. 6. Passenger mode: (a) perspective in VR and (b) user; Driver mode: (c) perspective in VR and (d) user with controller.

Participants completed the calibration process, and could optionally reduce the overall intensity to 90% or 80% based on personal preference. After calibration, participants completed all four tasks, each consisted of three conditions in counter-balanced ordering. Participants rested for a few minutes between each condition to make sure that they felt no discomfort before the next trial. Participants could terminate the experiment at any time due to discomfort.

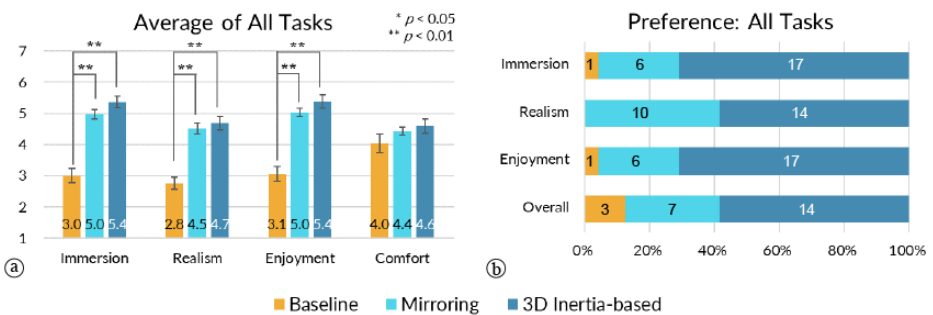


Fig. 7. (a) Average scores of immersion, realism, enjoyment, and comfort on a 7-point Likert scale. This figure shows the scores averaged from the four tasks. Error bars represent SEM. (b) Preference ranking among all tasks. The two feedback designs are preferred by at least 88% of the participants for comfort, realism, enjoyment, and immersion. The 3D *inertia-based* condition is the most preferable.

### 5.3 Analysis of Results

To compare the Likert ratings across three conditions, we first performed Friedman test then with Wilcoxon tests for pairwise post hoc analysis, with Bonferroni correction applied. Effect size of each comparison is calculated as  $r = \frac{Z}{\sqrt{N}}$  [53].

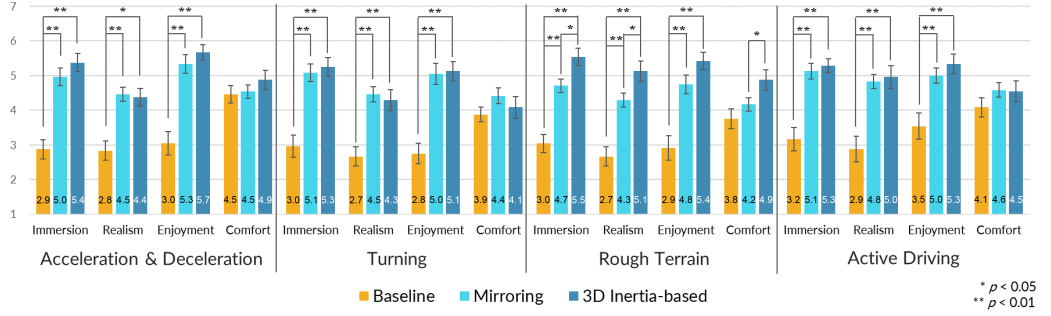


Fig. 8. Average ratings of immersion, realism, enjoyment, and comfort on a 7-point Likert scale for each task. Error bars represent SEM.

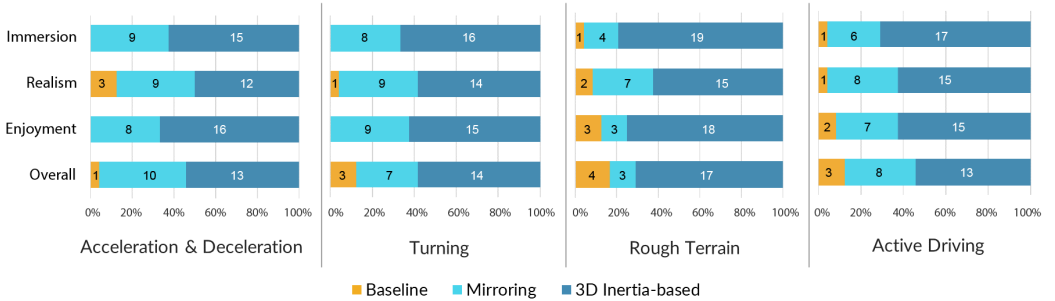


Fig. 9. Preference ranking of immersion, realism, enjoyment, and overall preference for each task.

### 5.3.1 Likert-scale Ratings: Overall.

Figure 7(a) shows the 7-point Likert-scale ratings averaged across all 4 tasks, showing that DrivingVibe designs have much higher ratings than the baseline for immersion, realism, and enjoyment. The *3D inertia-based* design had the highest ratings for all four dimensions, followed by the *mirroring* design, followed by the baseline.

Friedman tests show statistically significant differences between all the conditions in terms of immersion, realism, and enjoyment ( $p < .00001$  for all), but no significance for comfort. Pairwise comparison showed significant improvement for both DrivingVibe designs vs. baseline for immersion, realism, and enjoyment ( $p < .01$  for all) with large effect sizes. However, no significant difference was found between the two DrivingVibe designs.

### 5.3.2 Likert-scale Ratings: By Task.

Figure 8 shows the Likert-scale ratings for each of the 4 tasks. The statistically significant findings are generally consistent with the overall finding, that there was a significant improvement for both DrivingVibe designs vs. baseline for immersion, realism, and enjoyment ( $p < .01$  for all) with large effect sizes.

Interestingly, it also shows that for the Rough Terrain task, the *3D inertia-based* design significantly improved immersion, realism, and comfort vs. the *mirroring* design ( $p < .05$  for all), all with large effect sizes.

### 5.3.3 Preference Ranking.

At the end of the study, after completing all tasks and conditions, participants were asked for their most preferred condition. As shown in 7(b), all participants preferred DrivingVibe over the baseline for realism (100%), with 96% for immersion and enjoyment, and 88% overall. Among those who preferred DrivingVibe, the *3D inertia-based* design was preferred for immersion (74%), realism (58%) and enjoyment (74%), and overall (66%). Figure 9 shows similar preference of *3D inertia-based* for each task.

### 5.3.4 Qualitative Feedback.

All participants in our study have real-life driving experience, and most participants who rated higher realism in the DrivingVibe designs reported that they could associate vibration patterns with their past experience. All participants reported that the haptic feedback they received felt like real life driving experience in most driving events.

Although DrivingVibe designs can significantly improve the experience for most participants, some participants do not find clear differences between *mirroring* and *3D inertia-based* designs. Some participants reported “I think mirroring and 3D inertia-based are similar” (P1/3/5/6/13) in at least one driving event. Some participants relied on the feedback intensity to evaluate the vibrotactile feedback. Participants(P1/P12/P17/P18/P19/P22/P24) reported that the intensity of either mirroring or 3D inertia-based approach was either too big or too small, and some of them expressed a preference for the other approach as being more realistic. However, there was no consistent trend in the participants’ perceptions of the intensity between the two approaches. Nonetheless, the intensity was used as a criterion for their preference.

Regarding the *3D inertia-based* design, directionality is an essential factor that affects the experience. 15 out of 24 participants noticed the directionality with the *3D inertia-based* design, and all of them thought the directionality improves the experience. Some participants found the vibration pattern and reported that “It feels like the feeling of inertia.” (P2/9). “Directionality makes me more comfortable.” (P2/3) and “Directional vibration makes me turn my head.” (P2, P10) are also notable replies. It shows that the inertia feedback might also be a cue to tell participants the turning directions.

Except for the first two tasks where the *3D inertia-based* approach took the main part, directional feedback also provides benefits in simulating driving on rough terrain. For instance, in interviews, participants reported experiences such as “I can clearly feel the vibration of a single tire entering the grass field” (P6/7) and “I can feel the bumpiness in different directions” (P9/10), which demonstrate how directionality affects the user experience. Directionality also allows us to provide participants with a more detailed haptic experience. In both feedback designs, the vibration occurs continuously when the participants drive on rough terrain. However, in the *3D inertia-based* design, we restrict the feedback area to the four corners, whereas in the *mirroring* design, participants experience long-term vibrations all over the head. Some participants reported issues with the *mirroring* design, such as “I received excessive vibration when the car passes slightly over the rough terrain” (P5/12/17/18), “I received vibration around the head, but the constant vibration on the forehead is uncomfortable and unwarranted” (P22/23), and “The vibration is intermittent and weird” (P19/21). Therefore, incorporating directional feedback into our haptic design can create more detailed and nuanced feedback, potentially improving user experiences.

## 6 DISCUSSION AND FUTURE DIRECTIONS

### 6.1 Pros and Cons of the Two DrivingVibe Approaches

The study results showed that both DrivingVibe designs are effective in enhancing the VR driving experience, and that *3D inertia-based* design, which provides directional feedback, was preferred 2:1 overall compared to *mirroring* (14 vs. 7 participants). In particular, the improvement was statistically significant for the realism, immersion, and comfort Likert-scale ratings for the rough terrain experience, which was preferred nearly 6:1 overall compared to *mirroring* (17 vs. 3 participants).

The two DrivingVibe approaches are complementary, in that *mirroring* supports all games that support vibrotactile feedback via controllers/gamepads/steering wheels, albeit at lower feedback fidelity, while *3D inertia-based* approach provides higher feedback fidelity for games that export telemetry data to motion platforms. To provide a sense of the difference in the number of games supported, there are currently 442 VR driving games on the SteamVR store that can be supported by *mirroring*, while two of the most popular motion platforms, Motion Systems and Next Level Racing, support a combined total of 77 games (both VR and non-VR).

### 6.2 Improving Vibration Patterns

User feedback on apparent tactile motion (ATM) used during *cold start* showed that only 4 out of 24 participants reported the design as intuitive, with 9 participants noticing it but did not interpret it as a continuous motion sensation, while 11 participants did not perceive ATM. This suggests that more exploration is needed to use ATM effectively for motion simulation. Specifically, the timing and intensity settings for rendering ATM may require calibration per person during device setup to ensure that all users can perceive ATM. Also, we plan to explore how the speed of ATM can be better designed to match the visual-induced and user-expected motion sensations.

Also, our current intensity mapping uses linear functions, but the perception of motion signals intensity may be improved using non-linear curves. For example, a logistic curve that emphasizes the low level more may be more effective in conveying the changes in motion when the magnitude of inertia forces is low.

### 6.3 Extending DrivingVibe to Other VR Experiences

While the scope of this paper focused on driving experience, the concept of 3D inertia-based design and the lessons learned may extend to other motion experiences, such as flight simulation and virtual sports such as skateboarding. The new challenges are designing feedback for scenarios that have additional degrees of freedom (DoF) compared to driving, such as flight simulation and riding roller coasters, which have common roll and pitch rotations. TurnAhead [33] addressed (3-DoF) rotational feedback by using air jets to generate shear forces via VR headsets. For vibrotactile-based feedback, additional actuators will likely be required to provide feedback for these additional, rotational DoFs, similar to the hardware design of HapticHead [29, 31] that provide spherical coverage.

### 6.4 Extending DrivingVibe to Other Parts of the Body

Three study participants suggested that the vibrotactile feedback be extended to additional body parts, including the torso and arms, similar to how motion platforms provide full-body motion simulation. One expansion approach will be replicating the ring-shaped feedback device for other parts of the body, such as a vibrotactile belt or vest, which may utilize the same inertia-based patterns. Another approach may utilize prior research that has demonstrated apparent tactile motion for other parts of the body, such as the back [26, 27], wrist [20], or forearm [26], to support more

degrees of freedom of apparent tactile motion. As an example, applying tactile motion vertically may improve the experience of vertical motion, such as hitting road bumps or even free fall experiences.

## 7 CONCLUSION

We presented DrivingVibe which explored two designs of vibrotactile feedback patterns around the head to enhance virtual driving experiences. User experience evaluation ( $n=24$ ) showed significant improvement in realism, immersion, and enjoyment, and that the majority of participants (88%) preferred DrivingVibe, with a 2:1 preference for 3D inertia-based vs. mirroring designs (14 vs. 7 participants). Comfort improved only in the rough terrain experience and not for other motion events, which motivates further exploration of designs that may improve comfort while reducing motion sickness [41]. To the best of our knowledge, this work is the first to design headset-based vibrotactile patterns for VR driving experiences. By open-sourcing this project, we hope to inspire others to explore haptic feedback designs for additional motion experiences, such as flight simulation.

## ACKNOWLEDGMENTS

This work was partially supported by the National Science and Technology Council, Taiwan, under grant NSTC 111-2221-E-011-133-, 111-2222-E-002-014 and 108-2628-E-002-006.

## REFERENCES

- [1] Max Baarspul. 1990. A review of flight simulation techniques. *Progress in Aerospace Sciences* 27, 1 (1990), 1–120.
- [2] Steven Beard, Estela Buchmann, Leslie Ringo, Thomas Tanita, and Brian Mader. 2008. Space shuttle landing and rollout training at the vertical motion simulator. In *AIAA Modeling and Simulation Technologies Conference and Exhibit*. 6541.
- [3] bHaptics. 2019. bHaptics Tactal. <https://www.bhaptics.com/tactsuit/tactal>
- [4] Harold E Burtt. 1917. Tactual illusions of movement. *Journal of Experimental Psychology* 2, 5 (1917), 371.
- [5] Hong-Yu Chang, Wen-Jie Tseng, Chia-En Tsai, Hsin-Yu Chen, Roshan Lalitha Peiris, and Liwei Chan. 2018. FacePush: Introducing Normal Force on Face with Head-Mounted Displays. In *Proceedings of the 31st Annual ACM Symposium on User Interface Software and Technology* (Berlin, Germany) (UIST '18). Association for Computing Machinery, New York, NY, USA, 927–935. <https://doi.org/10.1145/3242587.3242588>
- [6] Taizhou Chen, Yi-Shiun Wu, and Kening Zhu. 2018. Investigating Different Modalities of Directional Cues for Multi-Task Visual-Searching Scenario in Virtual Reality. In *Proceedings of the 24th ACM Symposium on Virtual Reality Software and Technology* (Tokyo, Japan) (VRST '18). Association for Computing Machinery, New York, NY, USA, Article 41, 5 pages. <https://doi.org/10.1145/3281505.3281516>
- [7] Shao-Yu Chu, Yun-Ting Cheng, Shih-Chin Lin, Yung-Wen Huang, Yi Chen, and Mike Y. Chen. 2021. MotionRing: Creating Illusory Tactile Motion around the Head using 360° Vibrotactile Headbands. In *Proceedings of the 34st Annual ACM Symposium on User Interface Software and Technology*.
- [8] Mark Colley, Pascal Jansen, Enrico Rukzio, and Jan Gugenheimer. 2022. SwiVR-Car-Seat: Exploring Vehicle Motion Effects on Interaction Quality in Virtual Reality Automated Driving Using a Motorized Swivel Seat. *Proc. ACM Interact. Mob. Wearable Ubiquitous Technol.* 5, 4, Article 150 (dec 2022), 26 pages. <https://doi.org/10.1145/3494968>
- [9] Fabien Danieau, Julien Fleureau, Philippe Guillotel, Nicolas Mollet, Anatole Lécuyer, and Marc Christie. 2012. HapSeat: Producing Motion Sensation with Multiple Force-Feedback Devices Embedded in a Seat. In *Proceedings of the 18th ACM Symposium on Virtual Reality Software and Technology* (Toronto, Ontario, Canada) (VRST '12). Association for Computing Machinery, New York, NY, USA, 69–76. <https://doi.org/10.1145/2407336.2407350>
- [10] Leo Hnatek Dennis Wolf, Michael Rietzler and Enrico Rukzio. 2019. Face/On: Multi-Modal Haptic Feedback for Head-Mounted Displays in Virtual Reality. *IEEE Transactions on Visualization and Computer Graphics* 25, 11 (11 2019), 3169–3177. <https://doi.org/10.1109/TVCG.2019.2932215>
- [11] Vincent Diener, Michael Beigl, Matthias Budde, and Erik Pescara. 2017. VibrationCap: Studying Vibrotactile Localization on the Human Head with an Unobtrusive Wearable Tactile Display. In *Proceedings of the 2017 ACM International Symposium on Wearable Computers* (Maui, Hawaii) (ISWC '17). Association for Computing Machinery, New York, NY, USA, 82–89. <https://doi.org/10.1145/3123021.3123047>
- [12] Huong Q Dinh, Neff Walker, Larry F Hodges, Chang Song, and Akira Kobayashi. 1999. Evaluating the importance of multi-sensory input on memory and the sense of presence in virtual environments. In *Proceedings IEEE Virtual Reality (Cat. No. 99CB36316)*. IEEE, 222–228.

- [13] Sony Electronics. 2023. PlayStationVR2. <https://www.playstation.com/en-us/ps-vr2/>
- [14] US Center for Disease Control and Prevention (CDC). [n. d.]. What Noises Cause Hearing Loss? [https://www.cdc.gov/nceh/hearing\\_loss/what\\_noises\\_cause\\_hearing\\_loss.html](https://www.cdc.gov/nceh/hearing_loss/what_noises_cause_hearing_loss.html)
- [15] Lawrence H. Frank, John G. Casali, and Walter W. Wierwille. 1988. Effects of Visual Display and Motion System Delays on Operator Performance and Uneasiness in a Driving Simulator. *Human Factors* 30, 2 (1988), 201–217. <https://doi.org/10.1177/001872088803000207> arXiv:<https://doi.org/10.1177/001872088803000207> PMID: 3384446.
- [16] Riku Fukuyama and Wataru Wakita. 2021. An Interactive Flight Operation with 2-DOF Motion Platform. In *Proceedings of the 27th ACM Symposium on Virtual Reality Software and Technology* (Osaka, Japan) (VRST '21). Association for Computing Machinery, New York, NY, USA, Article 56, 2 pages. <https://doi.org/10.1145/3489849.3489911>
- [17] J. M. Goldberg and C. Fernandez. 1975. Responses Of Peripheral Vestibular Neurons To Angular And Linear Accelerations In The Squirrel Monkey. *Acta Oto-Laryngologica* 80, 1-6 (1975), 101–110. <https://doi.org/10.3109/00016487509121307> arXiv:<https://doi.org/10.3109/00016487509121307>
- [18] John F Golding. 1998. Motion sickness susceptibility questionnaire revised and its relationship to other forms of sickness. *Brain Research Bulletin* 47, 5 (1998), 507 – 516. [https://doi.org/10.1016/S0361-9230\(98\)00091-4](https://doi.org/10.1016/S0361-9230(98)00091-4)
- [19] Jan Gugenheimer, Dennis Wolf, Eythor R. Eiriksson, Pattie Maes, and Enrico Rukzio. 2016. GyroVR: Simulating Inertia in Virtual Reality using Head Worn Flywheels. In *Proceedings of the 29th Annual Symposium on User Interface Software and Technology*.
- [20] Aakar Gupta, Thomas Pietrzak, Nicolas Roussel, and Ravin Balakrishnan. 2016. *Direct Manipulation in Tactile Displays*. Association for Computing Machinery, New York, NY, USA, 3683–3693. <https://doi.org/10.1145/2858036.2858161>
- [21] Sangyo Han, Sunung Mun, Jongman Seo, Jaebong Lee, and Seungmoon Choi. 2018. 4D Experiences Enabled by Automatic Synthesis of Motion and Vibrotactile Effects. In *Extended Abstracts of the 2018 CHI Conference on Human Factors in Computing Systems* (Montreal QC, Canada) (CHI EA '18). Association for Computing Machinery, New York, NY, USA, 1–4. <https://doi.org/10.1145/3170427.3186516>
- [22] Peter A Hancock, Dennis A Vincenzi, John A Wise, and Mustapha Mouloua. 2008. *Human factors in simulation and training*. CRC Press.
- [23] Philipp Hock, Mark Colley, Ali Askari, Tobias Wagner, Martin Baumann, and Enrico Rukzio. 2022. Introducing VAMPIRE – Using Kinaesthetic Feedback in Virtual Reality for Automated Driving Experiments. In *Proceedings of the 14th International Conference on Automotive User Interfaces and Interactive Vehicular Applications* (Seoul, Republic of Korea) (AutomotiveUI '22). Association for Computing Machinery, New York, NY, USA, 204–214. <https://doi.org/10.1145/3543174.3545252>
- [24] Matthias Hoppe, Daria Oskina, Albrecht Schmidt, and Thomas Kosch. 2021. Odin's Helmet: A Head-Worn Haptic Feedback Device to Simulate G-Forces on the Human Body in Virtual Reality. *Proc. ACM Hum.-Comput. Interact.* 5, EICS, Article 212 (May 2021), 15 pages. <https://doi.org/10.1145/3461734>
- [25] Juro Hosoi, Yuki Ban, Kenichi Ito, and Shin'ichi Warisawa. 2021. VWind: Virtual Wind Sensation to the Ear by Cross-Modal Effects of Audio-Visual, Thermal, and Vibrotactile Stimuli. In *SIGGRAPH Asia 2021 Emerging Technologies* (Tokyo, Japan) (SA '21 Emerging Technologies). Association for Computing Machinery, New York, NY, USA, Article 18, 2 pages. <https://doi.org/10.1145/3476122.3484848>
- [26] Ali Israr and Ivan Poupyrev. 2011. Control space of apparent haptic motion. In *2011 IEEE World Haptics Conference*. 457–462. <https://doi.org/10.1109/WHC.2011.5945529>
- [27] Ali Israr and Ivan Poupyrev. 2011. Tactile Brush: Drawing on Skin with a Tactile Grid Display. In *Proceedings of the SIGCHI Conference on Human Factors in Computing Systems* (Vancouver, BC, Canada) (CHI '11). Association for Computing Machinery, New York, NY, USA, 2019–2028. <https://doi.org/10.1145/1978942.1979235>
- [28] Oliver Beren Kaul and Michael Rohs. 2016. HapticHead: 3D Guidance and Target Acquisition through a Vibrotactile Grid. In *Proceedings of the 2016 CHI Conference Extended Abstracts on Human Factors in Computing Systems* (San Jose, California, USA) (CHI EA '16). Association for Computing Machinery, New York, NY, USA, 2533–2539. <https://doi.org/10.1145/2851581.2892355>
- [29] Oliver Beren Kaul and Michael Rohs. 2017. HapticHead: A Spherical Vibrotactile Grid around the Head for 3D Guidance in Virtual and Augmented Reality. In *Proceedings of the 2017 CHI Conference on Human Factors in Computing Systems* (Denver, Colorado, USA) (CHI '17). Association for Computing Machinery, New York, NY, USA, 3729–3740. <https://doi.org/10.1145/3025453.3025684>
- [30] Oliver Beren Kaul, Michael Rohs, and Marc Mogalle. 2020. Design and Evaluation of On-the-Head Spatial Tactile Patterns. In *19th International Conference on Mobile and Ubiquitous Multimedia* (Essen, Germany) (MUM '20). Association for Computing Machinery, New York, NY, USA, 229–239. <https://doi.org/10.1145/3428361.3428407>
- [31] Oliver Beren Kaul, Michael Rohs, Marc Mogalle, and Benjamin Simon. 2021. Around-the-Head Tactile System for Supporting Micro Navigation of People with Visual Impairments. *ACM Trans. Comput.-Hum. Interact.* 28, 4, Article 27 (jul 2021), 35 pages. <https://doi.org/10.1145/3458021>

- [32] Oliver Beren Kaul, Michael Rohs, Benjamin Simon, Kerem Can Demir, and Kamillo Ferry. 2020. Vibrotactile Funneling Illusion and Localization Performance on the Head. In *Proceedings of the 2020 CHI Conference on Human Factors in Computing Systems* (Honolulu, HI, USA) (*CHI '20*). Association for Computing Machinery, New York, NY, USA, 1–13. <https://doi.org/10.1145/3313831.3376335>
- [33] Bo-Cheng Ke, Min-Han Li, Yu Chen, Chia-Yu Cheng, Chiao-Ju Chang, Yun-Fang Li, Shun-Yu Wang, Chiao Fang, and Mike Y. Chen. 2023. TurnAhead: Designing 3-DoF Rotational Haptic Cues to Improve First-Person Viewing (FPV) Experiences. In *Proceedings of the 2023 CHI Conference on Human Factors in Computing Systems* (Hamburg, Germany) (*CHI '23*). Association for Computing Machinery, New York, NY, USA, Article 401, 15 pages. <https://doi.org/10.1145/3544548.3581443>
- [34] Konstantina Kilteni, Jean-Marie Normand, Maria V Sanchez-Vives, and Mel Slater. 2012. Extending body space in immersive virtual reality: a very long arm illusion. *PLoS one* 7, 7 (2012), e40867.
- [35] Jiwan Lee, Jaejun Park, and Seungmoon Choi. 2021. Absolute and Differential Thresholds of Motion Effects in Cardinal Directions. In *Proceedings of the 27th ACM Symposium on Virtual Reality Software and Technology* (Osaka, Japan) (*VRST '21*). Association for Computing Machinery, New York, NY, USA, Article 34, 10 pages. <https://doi.org/10.1145/3489849.3489870>
- [36] Beomsu Lim, Sangyoon Han, and Seungmoon Choi. 2021. Image-Based Texture Styling for Motion Effect Rendering. In *Proceedings of the 27th ACM Symposium on Virtual Reality Software and Technology* (Osaka, Japan) (*VRST '21*). Association for Computing Machinery, New York, NY, USA, Article 20, 10 pages. <https://doi.org/10.1145/3489849.3489854>
- [37] Shi-Hong Liu, Pai-Chien Yen, Yi-Hsuan Mao, Yu-Hsin Lin, Erick Chandra, and Mike Y. Chen. 2020. HeadBlaster: A Wearable Approach to Simulating Motion Perception Using Head-Mounted Air Propulsion Jets. *ACM Trans. Graph.* 39, 4, Article 84 (July 2020), 12 pages. <https://doi.org/10.1145/3386569.3392482>
- [38] Kim Ly, Pascal Karg, Julian Kreimeier, and Timo Götzemann. 2022. Development and Evaluation of a Low-Cost Wheelchair Simulator for the Haptic Rendering of Virtual Road Conditions. In *Proceedings of the 15th International Conference on Pervasive Technologies Related to Assistive Environments* (Corfu, Greece) (*PETRA '22*). Association for Computing Machinery, New York, NY, USA, 32–39. <https://doi.org/10.1145/3529190.3529195>
- [39] S. Mack, E.R. Kandel, T.M. Jessell, J.H. Schwartz, S.A. Siegelbaum, and A.J. Hudspeth. 2013. *Principles of Neural Science, Fifth Edition*. McGraw-Hill Education. <https://books.google.com.tw/books?id=s64z-LdAIsEC>
- [40] Berning Matthias, Braun Florian, Riedel Till, and Beigl Michael. 2015. ProximityHat: a head-worn system for subtle sensory augmentation with tactile stimulation. In *Proceedings of the 2015 ACM International Symposium on Wearable Computers - ISWC '15*. ACM Press, 31 – 38. <https://doi.org/10.1145/2802083.2802088>
- [41] Andrii Matvienko, Florian Müller, Marcel Zickler, Lisa Alina Gasche, Julia Abels, Till Steinert, and Max Mühlhäuser. 2022. Reducing Virtual Reality Sickness for Cyclists in VR Bicycle Simulators. In *Proceedings of the 2022 CHI Conference on Human Factors in Computing Systems* (New Orleans, LA, USA) (*CHI '22*). Association for Computing Machinery, New York, NY, USA, Article 187, 14 pages. <https://doi.org/10.1145/3491102.3501959>
- [42] Thomas Muender, Michael Bonfert, Anke Verena Reinschluessel, Rainer Malaka, and Tanja Döring. 2022. Haptic Fidelity Framework: Defining the Factors of Realistic Haptic Feedback for Virtual Reality. In *Proceedings of the 2022 CHI Conference on Human Factors in Computing Systems* (New Orleans, LA, USA) (*CHI '22*). Association for Computing Machinery, New York, NY, USA, Article 431, 17 pages. <https://doi.org/10.1145/3491102.3501953>
- [43] Kimberly Myles, Joel T. Kalb, Janea Lowery, and Bheem P. Kattel. 2015. The effect of hair density on the coupling between the tactus and the skin of the human head. *Applied Ergonomics* 48 (2015), 177 – 185. <https://doi.org/10.1016/j.apergo.2014.11.007>
- [44] Fumihiro Nakamura, Adrien Verhulst, Kuniharu Sakurada, Masaaki Fukuoka, and Maki Sugimoto. 2021. Virtual Whiskers: Cheek Haptic-Based Spatial Directional Guidance in a Virtual Space. In *SIGGRAPH Asia 2021 XR* (Tokyo, Japan) (*SA '21 XR*). Association for Computing Machinery, New York, NY, USA, Article 17, 2 pages. <https://doi.org/10.1145/3478514.3487625>
- [45] Arshad Nasser, Kexin Zheng, and Kening Zhu. 2021. ThermEarhook: Investigating Spatial Thermal Haptic Feedback on the Auricular Skin Area. In *Proceedings of the 2021 International Conference on Multimodal Interaction* (Montréal, QC, Canada) (*ICMI '21*). Association for Computing Machinery, New York, NY, USA, 662–672. <https://doi.org/10.1145/3462244.3479922>
- [46] Eric Jalbert Nefarius, Kanuan. 2020. Virtual Gamepad Emulation Framework. <https://github.com/ViGEM>
- [47] Yi-Hao Peng, Carolyn Yu, Shi-Hong Liu, Chung-Wei Wang, Paul Taele, Neng-Hao Yu, and Mike Y. Chen. 2020. WalkingVibe: Reducing Virtual Reality Sickness and Improving Realism While Walking in VR Using Unobtrusive Head-Mounted Vibrotactile Feedback. Association for Computing Machinery, New York, NY, USA, 1–12. <https://doi.org/10.1145/3313831.3376847>
- [48] D. Pittera, D. Ablart, and M. Obrist. 2019. Creating an Illusion of Movement between the Hands Using Mid-Air Touch. *IEEE Trans Haptics* 12, 4 (2019), 615–623.

- [49] Nimesha Ranasinghe, Pravar Jain, Shienny Karwita, David Tolley, and Ellen Yi-Luen Do. 2017. Ambiotherm: Enhancing Sense of Presence in Virtual Reality by Simulating Real-World Environmental Conditions. In *Proceedings of the 2017 CHI Conference on Human Factors in Computing Systems* (Denver, Colorado, USA) (*CHI '17*). Association for Computing Machinery, New York, NY, USA, 1731–1742. <https://doi.org/10.1145/3025453.3025723>
- [50] Markus Rank, Zhuanghua Shi, Hermann J. Müller, and Sandra Hirche. 2010. Perception of Delay in Haptic Telepresence Systems. *Presence: Teleoperators and Virtual Environments* 19, 5 (10 2010), 389–399. [https://doi.org/10.1162/pres\\_a\\_00021](https://doi.org/10.1162/pres_a_00021) arXiv:[https://direct.mit.edu/pvar/article-pdf/19/5/389/1621619/pres\\_a\\_00021.pdf](https://direct.mit.edu/pvar/article-pdf/19/5/389/1621619/pres_a_00021.pdf)
- [51] Michael Rietzler, Katrin Plaumann, Taras Kränzle, Marcel Erath, Alexander Stahl, and Enrico Rukzio. 2017. VaiR: Simulating 3D Airflows in Virtual Reality. In *Proceedings of the 2017 CHI Conference on Human Factors in Computing Systems* (Denver, Colorado, USA) (*CHI '17*). Association for Computing Machinery, New York, NY, USA, 5669–5677. <https://doi.org/10.1145/3025453.3026009>
- [52] John M Rolfe and Ken J Staples. 1988. *Flight simulation*. Number 1. Cambridge University Press.
- [53] Robert Rosenthal, Harris Cooper, Larry Hedges, et al. 1994. Parametric measures of effect size. *The handbook of research synthesis* 621, 2 (1994), 231–244.
- [54] James Schelter and Frank Masi. 1998. Theater with seat and wheelchair platform movement. US Patent 5,829,201.
- [55] Jongman Seo, Sunung Mun, Jaebong Lee, and Seungmoon Choi. 2018. Substituting Motion Effects with Vibrotactile Effects for 4D Experiences. In *Proceedings of the 2018 CHI Conference on Human Factors in Computing Systems* (Montreal QC, Canada) (*CHI '18*). Association for Computing Machinery, New York, NY, USA, 1–6. <https://doi.org/10.1145/3173574.3174002>
- [56] Vivian Shen, Craig Shultz, and Chris Harrison. 2022. Mouth Haptics in VR Using a Headset Ultrasound Phased Array. In *Proceedings of the 2022 CHI Conference on Human Factors in Computing Systems* (New Orleans, LA, USA) (*CHI '22*). Association for Computing Machinery, New York, NY, USA, Article 275, 14 pages. <https://doi.org/10.1145/3491102.3501960>
- [57] Solla. 2021. Variable-LRA-Frequencies-on-DRV2605. <https://github.com/Solla/Variable-LRA-Frequencies-on-DRV2605>
- [58] Doug Stewart. 1965. A platform with six degrees of freedom. *Proceedings of the institution of mechanical engineers* 180, 1 (1965), 371–386.
- [59] Yudai Tanaka, Jun Nishida, and Pedro Lopes. 2022. Demonstrating Electrical Head Actuation: Enabling Interactive Systems to Directly Manipulate Head Orientation. In *Extended Abstracts of the 2022 CHI Conference on Human Factors in Computing Systems* (New Orleans, LA, USA) (*CHI EA '22*). Association for Computing Machinery, New York, NY, USA, Article 182, 5 pages. <https://doi.org/10.1145/3491101.3519904>
- [60] Yudai Tanaka, Jun Nishida, and Pedro Lopes. 2022. Electrical Head Actuation: Enabling Interactive Systems to Directly Manipulate Head Orientation. In *Proceedings of the 2022 CHI Conference on Human Factors in Computing Systems* (New Orleans, LA, USA) (*CHI '22*). Association for Computing Machinery, New York, NY, USA, Article 262, 15 pages. <https://doi.org/10.1145/3491102.3501910>
- [61] Taku Tanichi, Futa Asada, Kento Matsuda, Danny Hynds, and Kouta Minamizawa. 2020. KABUTO: Inducing Upper-Body Movements Using a Head Mounted Haptic Display with Flywheels. In *SIGGRAPH Asia 2020 Emerging Technologies* (Virtual Event, Republic of Korea) (*SA '20*). Association for Computing Machinery, New York, NY, USA, Article 9, 2 pages. <https://doi.org/10.1145/3415255.3422880>
- [62] Chun-Miao Tseng, Po-Yu Chen, Shih Chin Lin, Yu-Wei Wang, Yu-Hsin Lin, Mu-An Kuo, Neng-Hao Yu, and Mike Y. Chen. 2022. HeadWind: Enhancing Teleportation Experience in VR by Simulating Air Drag during Rapid Motion. In *Proceedings of the 2022 CHI Conference on Human Factors in Computing Systems* (New Orleans, LA, USA) (*CHI '22*). Association for Computing Machinery, New York, NY, USA, Article 518, 11 pages. <https://doi.org/10.1145/3491102.3501890>
- [63] A. Välijamäe, P. Larsson, D. Västfjäll, and M. Kleiner. 2005. Travelling without moving: Auditory scene cues for translational self-motion.
- [64] Dong-Bach Vo, Julia Saari, and Stephen Brewster. 2021. TactiHelm: Tactile Feedback in a Cycling Helmet for Collision Avoidance. In *Extended Abstracts of the 2021 CHI Conference on Human Factors in Computing Systems* (Yokohama, Japan) (*CHI EA '21*). Association for Computing Machinery, New York, NY, USA, Article 267, 5 pages. <https://doi.org/10.1145/3411763.3451580>
- [65] Chi Wang, Da-Yuan Huang, Shuo-wen Hsu, Chu-En Hou, Yeu-Luen Chiu, Ruei-Che Chang, Jo-Yu Lo, and Bing-Yu Chen. 2019. Masque: Exploring lateral skin stretch feedback on the face with head-mounted displays. In *Proceedings of the 32nd Annual ACM Symposium on User Interface Software and Technology*, 439–451.
- [66] Alexander Wilberz, Dominik Leschtschow, Christina Trepkowksi, Jens Maiero, Ernst Kruijff, and Bernhard Riecke. 2020. FaceHaptics: Robot Arm based Versatile Facial Haptics for Immersive Environments. In *Proceedings of the 2020 CHI Conference on Human Factors in Computing Systems*. ACM. <https://doi.org/10.1145/3313831.3376481>
- [67] Benjamin Williams, Alexandra E. Garton, and Christopher J. Headland. 2020. Exploring Visuo-haptic Feedback Congruency in Virtual Reality. In *2020 International Conference on Cyberworlds (CW)*, 102–109. <https://doi.org/10.1109/CW49994.2020.00022>

- [68] Bob G. Witmer, Christian J. Jerome, and Michael J. Singer. 2005. The Factor Structure of the Presence Questionnaire. *Presence: Teleoperators and Virtual Environments* 14, 3 (06 2005), 298–312. <https://doi.org/10.1162/105474605323384654> arXiv:<https://direct.mit.edu/pvar/article-pdf/14/3/298/1624394/105474605323384654.pdf>
- [69] Gyeore Yun, Hyoseung Lee, Sangyoon Han, and Seungmoon Choi. 2021. Improving Viewing Experiences of First-Person Shooter Gameplays with Automatically-Generated Motion Effects. In *Proceedings of the 2021 CHI Conference on Human Factors in Computing Systems* (Yokohama, Japan) (CHI ’21). Association for Computing Machinery, New York, NY, USA, Article 320, 14 pages. <https://doi.org/10.1145/3411764.3445358>

## A DETAILS OF THE USER STUDY RESULTS

This appendix includes the analysis statistics in all the pairwise comparison as well as the preferences rankings collected in each of the task in the user experience evaluation study.

For Friedman tests, we reported the  $p$ -value as well as the Kendall’s W value ( $W = \frac{\chi^2}{N(K-1)}$ ) as the effect size. For Wilcoxon tests, we used  $r = \frac{Z}{\sqrt{N}}$  as the effect size. Both effect size use the same interpretation guidelines of  $0.1 \sim 0.3$  (small effect),  $0.3 \sim 0.5$  (moderate effect), and  $\geq 0.5$  (large effect)

Table 1. Statistics of the analysis with the average scores among all tasks.

	$\chi^2_r$	$p$ -value	$W$	Pairwise Comparison	$Z$	$p$ -value	$r$
Immersion	39.52	$<0.00001$ **	0.82	Baseline < Mirroring	-4.29	$<0.00001$ **	0.87
				Baseline < Inertia	-4.29	$<0.00001$ **	0.87
				Mirroring < Inertia	-2.03	0.02118	0.44
Realism	31.00	0.00001 **	0.65	Baseline < Mirroring	-4.14	$<0.00001$ **	0.85
				Baseline < Inertia	-3.84	0.00006 **	0.78
				Mirroring < Inertia	-0.65	0.25785	0.14
Enjoyment	31.58	$<0.00001$ **	0.66	Baseline < Mirroring	-4.19	$<0.00001$ **	0.85
				Baseline < Inertia	-4.23	$<0.00001$ **	0.86
				Mirroring < Inertia	-1.47	0.07078	0.30
Comfort	3	0.22313	0.06	Baseline < Mirroring	—	—	—
				Baseline < Inertia	—	—	—
				Mirroring < Inertia	—	—	—

Table 2. Statistics of the analysis in task 1

	$\chi^2_r$	$p$ -value	$W$	Pairwise Comparison	$Z$	$p$ -value	$r$
Immersion	27.15	$<0.00001$ **	0.57	Baseline < Mirroring	-3.92	0.00004 **	0.88
				Baseline < Inertia	-4.01	$<0.00001$ **	0.88
				Mirroring < Inertia	-1.52	0.06426	0.36
Realism	18.15	0.00011 **	0.38	Baseline < Mirroring	-3.21	0.00066 **	0.66
				Baseline < Inertia	-2.69	0.00357 *	0.57
				Mirroring < Inertia	-0.40	0.34458	0.10
Enjoyment	28.31	$<0.00001$ **	0.59	Baseline < Mirroring	-4.01	$<0.00001$ **	0.88
				Baseline < Inertia	-4.01	$<0.00001$ **	0.88
				Mirroring < Inertia	-0.93	0.17619	0.23
Comfort	2.90	0.23506	0.06	Baseline < Mirroring	—	—	—
				Baseline < Inertia	—	—	—
				Mirroring < Inertia	—	—	—

Table 3. Statistics of the analysis in task 2

	$\chi^2_r$	p-value	W	Pairwise Comparison	Z	p-value	r
Immersion	25.52	<0.00001 **	0.53	Baseline < Mirroring	-3.92	0.00004 **	0.88
				Baseline < Inertia	-3.96	0.00004 **	0.84
				Mirroring < Inertia	-0.58	0.28096	0.13
Realism	17.15	0.00019 **	0.36	Baseline < Mirroring	-3.72	0.0001 **	0.88
				Baseline < Inertia	-3.16	0.00079 **	0.69
				Mirroring < Inertia	-0.57	0.28434	0.13
Enjoyment	26.69	<0.00001 **	0.56	Baseline < Mirroring	-4.01	<0.00001 **	0.88
				Baseline < Inertia	-3.92	0.00004 **	0.88
				Mirroring < Inertia	-0.18	0.42858	0.04
Comfort	1.08	0.58178	0.02	Baseline < Mirroring	-	-	-
				Baseline < Inertia	-	-	-
				Mirroring < Inertia	-	-	-

Table 4. Statistics of the analysis in task 3

	$\chi^2_r$	p-value	W	Pairwise Comparison	Z	p-value	r
Immersion	28.15	<0.00001 **	0.59	Baseline < Mirroring	-3.38	0.00036 **	0.72
				Baseline < Inertia	-4.08	<0.00001 **	0.88
				Mirroring < Inertia	-2.62	0.0044 *	0.60
Realism	19.31	0.00006 **	0.38	Baseline < Mirroring	-3.06	0.00111 **	0.64
				Baseline < Inertia	-3.71	0.0001 **	0.83
				Mirroring < Inertia	-2.27	0.0116 *	0.52
Enjoyment	16.90	0.00021 **	0.59	Baseline < Mirroring	-3.08	0.00104 **	0.69
				Baseline < Inertia	-3.67	0.00012 **	0.80
				Mirroring < Inertia	-2.07	0.01923	0.52
Comfort	7.75	0.02075 *	0.16	Baseline < Mirroring	-0.82	0.20611	0.18
				Baseline < Inertia	-2.00	0.02275	0.44
				Mirroring < Inertia	-2.30	0.01072 *	0.59

Received January 2023; revised May 2023; accepted June 2023

Table 5. Statistics of the analysis in task 4

	$\chi^2_r$	p-value	W	Pairwise Comparison	Z	p-value	r
Immersion	25.52	<0.00001 **	0.53	Baseline < Mirroring	-3.99	0.00003 **	0.85
				Baseline < Inertia	-3.61	0.00015 **	0.74
				Mirroring < Inertia	-1.22	0.11123	0.34
Realism	25.52	<0.00001 **	0.53	Baseline < Mirroring	-4.01	<0.00001 **	0.88
				Baseline < Inertia	-3.77	0.00008 **	0.79
				Mirroring < Inertia	-0.75	0.22663	0.19
Enjoyment	14.58	0.00068 **	0.30	Baseline < Mirroring	-3.36	0.00039 **	0.75
				Baseline < Inertia	-2.91	0.00181 **	0.65
				Mirroring < Inertia	-1.35	0.08851	0.32
Comfort	1.75	0.41686	0.04	Baseline < Mirroring	-	-	-
				Baseline < Inertia	-	-	-
				Mirroring < Inertia	-	-	-